Available online at www.sciencedirect.com
ScienceDirect
Journal of Solid State Chemistry 180 (2007) 2371–2376
JOURNAL OF SOLID STATE CHEMISTRY
www.elsevier.com/locate/jssc

Effects of firing schedule on solubility limits and transport properties of ZrO_2–TiO_2–Y_2O_3 fluorites

D.P. Fagg[a,*], J.R. Frade[a], M. Mogensen[b], J.T.S. Irvine[c]

[a]*Aveiro University, Aveiro, Portugal*
[b]*Risø National Laboratory, Roskilde, Denmark*
[c]*St. Andrews University, St. Andrews, Fife, Scotland*

Received 12 March 2007; received in revised form 12 June 2007; accepted 20 June 2007
Available online 26 June 2007

Abstract

The low Y/high Zr edge of the cubic defect fluorite solid solution in the system ZrO_2–TiO_2–Y_2O_3 in air is reassessed, as it is these compositions which have been suggested to offer the highest levels of mixed conductivity. Vegard's law is obeyed for values of x which lie within the cubic defect fluorite phase in $Zr_{1-x-y}Y_yTi_xO_{2-\delta}$ for values of $y = 0.2$ and 0.25. Measured lattice parameters show good agreement with those calculated from the Kim relation. Deviation from Vegard's law places the limit of the solid solution at $x = 0.18$ and 0.20 for values of $y = 0.2$ and 0.25, respectively, at 1500 °C. Discrepancies in current literature data can be shown to be due to differences in firing schedule such as slight temperature fluctuations and/or different cooling rates. A high level of care of sintering temperature and cooling profile is essential to form the most promising single-phase materials which contain maximum Ti-contents with low Y-contents. Contraction of the phase limit as a result of poor synthesis control leads to erroneously high values of bulk ionic conductivity while values of electronic conductivity are shown to be less affected.

Keywords: Fluorite; Mixed conductor; Phase limits; Solid solubility; Ionic conductivity

1. Introduction

Many fluorite-based oxides offer good oxide-ion conductivity and it is possible to dope these materials with small concentrations of variable valence ions, such as the early transition metals Ti and Nb, to produce a significant electronic contribution to the total conductivity when in reducing atmospheres. These materials have been suggested for use as solid oxide fuel cell (SOFC) anodes due to their excellent stability at high temperature, good compatibility with the YSZ electrolyte and reasonable electrocatalytic activity for the hydrogen oxidation reaction [1–5]. Unfortunately, previous work has shown that the magnitude of the ionic component is often impaired at the levels of doping required to achieve a reasonable electronic enhancement [3,6]. The general consensus is that, even though the total conductivity of these materials is too low for use as a 'stand alone' anode material, they have considerable potential for use in composite anodes, such as Ni–ZrO_2–TiO_2–Y_2O_3 cermets [7,8].

Much work has been done to assess the composition dependence of ionic conductivity within the defect fluorite solid solution of the system ZrO_2–TiO_2–Y_2O_3 [1–6,9–13]. The reported trends unequivocally support the trends observed in similar systems, such as, Zr(Nb,Ti)(Gd,Ca,Yb,Y)$O_{2-\delta}$ systems [6], where the electronic contribution to mixed conduction increases with the concentration of transition metal ions while the ionic conductivity is dominated by the concentration of the large rare-earth dopant, decreasing dramatically as concentration increases. At a constant rare-earth concentration, increases in transition element content lead to small decreases in both ionic conductivity and activation energy for conduction [6]. Therefore, for any fixed Ti-content the defect fluorite compositions offering the highest ionic conductivity will be those on the low Y/high Zr edge of the solid solution [3–6,9–13]. Unfortunately, the literature shows serious disagreement of the

*Corresponding author. Fax: +351 234 425300.
E-mail address: duncan@cv.ua.pt (D.P. Fagg).

0022-4596/$ - see front matter © 2007 Elsevier Inc. All rights reserved.
doi:10.1016/j.jssc.2007.06.016

limits of the solid solution for this edge of the ZrO_2–TiO_2–Y_2O_3 phase diagram, especially for low Y-contents close to those found in YSZ, and also disagreement with respect to levels of bulk ionic conductivity [1–6,9–14]. If we consider the join between TiO_2 and 8 mol% YSZ at 1500°C as one example, the phase diagram of Colomer et al. [12] places the solid solution limit at 18 mol% TiO_2, whereas the phase diagram of Feighery et al. [14] locates the limit at only 7 mol% TiO_2, in agreement with Traqueira [13]. Similar disparity is also noted in reported bulk ionic conductivities, e.g. variations of over an order of magnitude can be noted for composition 10 mol% TiO_2-8YSZ produced under identical sintering temperatures and from the same precursor powders [13,15]. In this work, the solubility of TiO_2 was carefully reassessed in compositions containing 20 and 25 mol% $YO_{1.5}$. These Y-contents were chosen as they allow significant Ti-contents ($\geqslant$0.15 mol% TiO_2) to be accommodated, hence promising levels of mixed conductivity are achieved, while still retaining the defect fluorite phase. Attempts were also made to offer possible explanations for the disparity in current literature data. Experimental lattice parameters were compared to theoretical parameters calculated using the empirical relation suggested by Kim [16] based on valence and ionic size differences, as this relation has previously been utilised by Yokokawa et al. [17] in full phase diagram calculations for the ternary system ZrO_2–$YO_{1.5}$–TiO_2. Hence, another aim of the current work was to experimentally determine the applicability of the Kim relationship for this ternary system.

2. Experimental

2.1. Sample preparation

Yttria, titania (Aldrich) and zircona (Tioxide) powders of purity 99.99%, were used as the starting materials. Y_2O_3 powder was calcined at 1000 °C and ZrO_2 and TiO_2 powders at 700 °C for 24 h. Powders were weighed directly from a desiccator to prevent moisture uptake. Stoichiometric amounts of these powders were intimately ground under acetone using an agate pestle and mortar and dry pressed into pellets under a pressure of 3 ton/cm^2. All powder weighed was included in the pellet for accuracy. Samples were fired in air at 1500 °C for 36 h followed by cooling to room temperature. Furnace temperature was accurately monitored by a thermocouple placed near the samples. Samples were either air quenched by dragging them into the furnace cold zone or slowly cooled. Phase purity and lattice parameter data were determined on crushed powder by X-ray diffraction using a Stoe Stadi-P diffractometer (stepwidth 0.02, 6 s per step); unit cell parameters were determined using a pseudo-Voight profile fit and an external silicon standard for zero point correction. Bulk ionic conductivity, determined on dense pellets using porous platinum paste electrodes, was separated by A.C. impedance spectroscopy. Typical spectra were dominated by the bulk impedance with no observable grain boundary response. The atmosphere dependence of total (ionic + electronic) conductivity was determined by A.C. impedance and performed in a controlled atmosphere furnace as described elsewhere [18]. All samples studied for electrical measurements had densities in the range 96–98% that of the theoretical density.

2.2. The Kim relation

The relation suggested by Kim [16] to estimate the composition dependence of lattice parameter for materials based on ZrO_2 is given by

$$a = 0.512 + \sum(0.0212\Delta r_k + 0.00023\Delta z_k)m_k,$$

where a (in nm) is the lattice constant of the ZrO_2 solid solution at room temperature, Δr_k (in nm) is the difference in ionic radius (r_k–r_h) of the kth dopant (r_k) and the host cation (r_h) in eight-fold coordination according to Shannon [19], Δz_k is the valency difference (z_k–z_h) and m_k is the mole percent of kth dopant in the form MO_x. This relation was empirically derived from literature data for binary ZrO_2–MO_x systems at low concentrations of dopant (<25 mol%). For higher dopant concentrations the fit of the Kim relation to experimental data is observed to be poor, showing increased deviation from true values as dopant concentration increases. This is exhibited in Fig. 1 for literature data on the system ZrO_2–$YO_{1.5}$ as an example

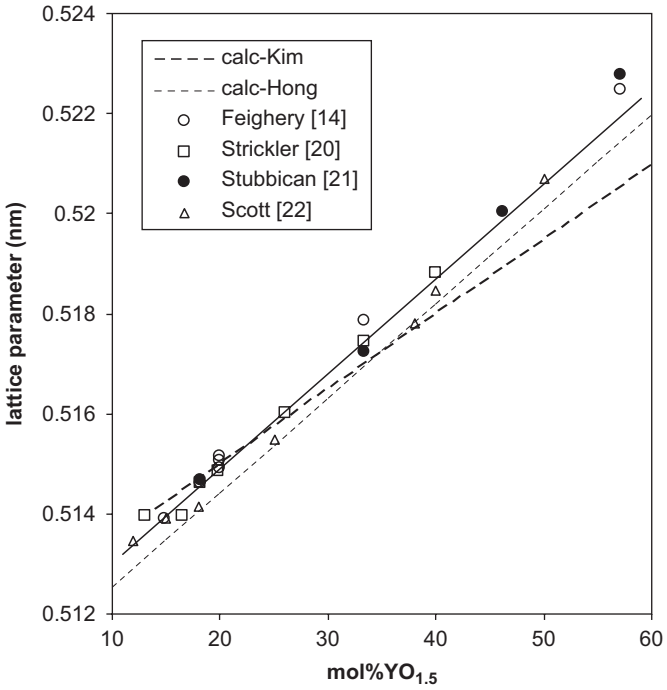

Fig. 1. Correlation of the Kim calculation with experimental data for the system ZrO_2–Y_2O_3. A poor fit is observed at higher dopant concentration. Solid line represents best fit of literature data, described by the equation $a = 1.9 \times 10^{-4}$ (mol% TiO_2) + 0.51109. Literature data is taken from the following references. Feighery et al. [14], Strickler and Carlson [20], Stubbican et al. [21], Scott [22].

[14,20–22]. The percentage error in the gradient predicted by Kim is approximately 20%. Hong and Virkar [23] provide an alternative relation with which to calculate lattice parameters of fluorite materials using the ionic radii and a concept of a specific radius for the oxygen vacancy. Their relationship provides a better estimation of lattice parameters for yttria-doped zirconia at high dopant concentrations (Fig. 1), but unfortunately cannot readily be transferred to predict lattice parameters for ternary oxides. In contrast, Kim suggests that his relation can be used to calculate lattice parameter data for ternary systems and examples are presented for the system ZrO_2–ThO_2–Y_2O_3, extending to a composition with 18.5 mol% ThO_2 and 3.5 mol% Y_2O_3, i.e. a composition which contains around 25 mol% dopants when stated in the form MO_x [16]. It is interesting to note that, even in this data presented by Kim, the relative error of the calculated lattice parameter for the ternary system increases as dopant concentration increases, especially when these dopants are aliovalent and of a large size mismatch with the host lattice; see Table 1 which reproduces this data. Despite this clear accuracy limitation of the Kim relationship at higher dopant concentrations, it has been utilised in full phase diagram calculations for the ternary systems ZrO_2–$YO_{1.5}$–MO_x where $MO_x = TiO_2$ and FeO_x by Yokokawa et al. [17] An assessment of the accuracy of the Kim relationship for these ternary systems is, therefore, imperative.

3. Results and discussion

3.1. $Zr_{0.8-x}Ti_xY_{0.2}O_{2-\delta}$ (20 mol% $YO_{1.5}$)

3.1.1. The extent of the cubic defect fluorite solid solution

The composition dependence of lattice parameter is shown in Fig. 2 for compositions containing 20 mol% $YO_{1.5}$ as a function of TiO_2 content. Literature data is included from Feighery et al. [14] and Liou and Worrell [2]. Lattice parameter is also calculated using the relation suggested by Kim [16].

Fig. 2 exhibits a reasonable correlation between the experimental results of the different authors. Previously, the data of Feighery et al. [14] were analysed by fitting to a curve. With more data now available in the low Ti range, it is clear that a linear fit better describes the data in this region. The lattice parameters calculated from the relation of Kim are in good agreement with the measured data in this low Ti concentration range. Such a good agreement between the Vegard's slope of the calculated and experimental data is perhaps somewhat surprising when we consider the previously mentioned accuracy restriction of the Kim relationship observed at high dopant concentrations. In this case, several factors assist the fit of the Kim equation. The Vegard's slope is dependent only on the concentration of the Ti dopant as the Y dopant concentration is fixed at 20 mol% $YO_{1.5}$ and in the Kim calculation the Y-content serves only to vary the value of lattice parameter which corresponds to the intercept at a Ti-content of zero. Second, both Ti and Zr have the same valency of 4+. The valency difference (z_{Zr}–z_{Ti}) of this

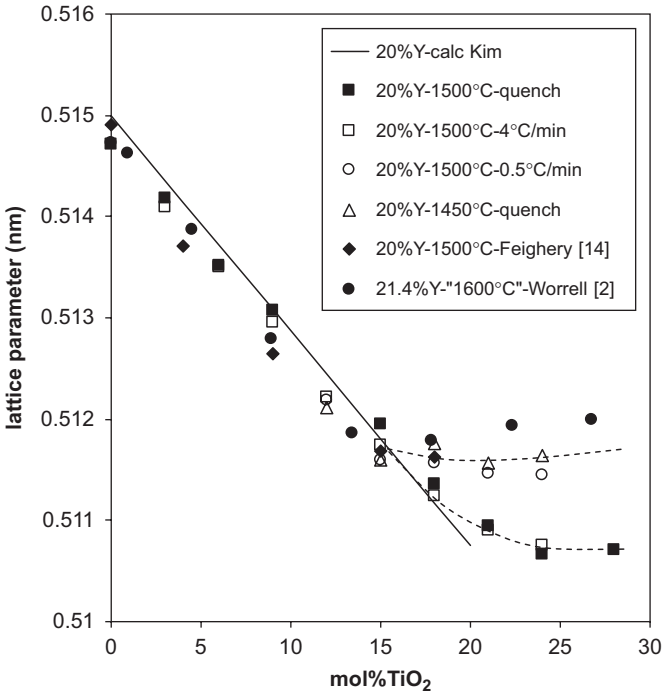

Fig. 2. The composition dependence of lattice parameter for compositions containing 20 mol% $YO_{1.5}$ as a function of Ti-content. Literature data is included from Feighery et al. [14] and Liou and Worrell [2] (21.4 mol% $YO_{1.5}$). Lattice parameter is also calculated using the relation suggested by Kim [16]. Processing conditions are shown in the legend.

Table 1
Calculated and experimental lattice parameters of compositions in the ternary system ZrO_2–ThO_2–$YO_{1.5}$ reported by Kim [16]

mol% ThO_2	mol% $YO_{1.5}$	Calculated lattice parameters (nm)	Experimental. lattice parameters (nm)	% Error	% Dopant MO_x
17.87	6.76	0.5210	0.5219	0.17	24.64
16.83	1.98	0.5198	0.5206	0.15	18.81
8.24	8.43	0.5164	0.5173	0.17	16.67
4.85	5.83	0.5150	0.5148	−0.04	10.68
0	16.51	0.5145	0.5142	−0.06	16.51

At elevated dopant concentrations, greater % errors are observed especially when dopants are aliovalent and of a large size mismatch for host lattice.

dopant, therefore, reduces to zero in the Kim equation to leave the gradient dependent solely on the term $0.0212(r_{Zr}-r_{Ti})$. Finally, the ionic radii of Ti^{4+} and Zr^{4+} in eight-fold coordination are comparable (0.074, 0.084 nm, respectively). Consequently, any slight error in the constant 0.0212 stated by Kim would, therefore, not lead to serious variations in Vegard's slope for the levels of Ti-content analysed here.

The limit of the cubic fluorite phase is given by the location of the break in Vegard's slope as Ti composition increases. In Fig. 2, the work by Liou and Worrell [2] and Feighery et al. [14] show a similar limit of the cubic fluorite solid solution at 15 mol% TiO_2; however, the new data show the limit to occur at 18 mol% TiO_2. Analysis of X-ray diffractograms taken for compositions beyond this phase limit show the presence of the secondary phase $Y_2Ti_2O_7$ in agreement with the phase diagram of Feighery et al. [14]. Assuming stoichiometric accuracy by all authors, the larger solid solution range in the present results could either be explained by a more efficient quenching mechanism or by furnace temperature variations between the experiments. In the current work, temperature was accurately monitored by a thermocouple placed near the samples during sintering at 1500 °C for 36 h followed by air quenching. In the work by Feighery et al. [14] samples were sintered in a muffle furnace at 1500 °C for 36 h and then air quenched, while in the work by Liou and Worrell [2] samples were sintered first at 1400 °C for 12 h then 1600 °C for 12 h followed by cooling for 24 h to room temperature (~1 °C/min). To test the former hypothesis, samples were reground and refired as powders at the same temperature as the first samples for 12 h but cooled slowly at 4 °C/min. Lattice parameters of the cubic phase of these samples are also plotted in Fig. 2. No significant change in lattice parameters could be induced by a change in sintering profile to 4 °C/min. However, repetition with a cooling rate of 0.5 °C/min leads to a significant change in lattice parameter and shrinkage of the extent of the solid solution, Fig. 2. Experiments to assess the importance of slight temperature variations on the solid solubility limit were performed by firing at the slightly lower temperature of 1450 °C and are summarised in Fig. 2. A small temperature variation of 50 °C is the type of temperature fluctuation that could result from the location of sample placement in a normal muffle furnace. Our results show that the influence of using a slow cooling rate of 0.5 °C/min or decreasing the sintering temperature by 50 °C appears to be equivalent, shrinking the solid solution to encompass the composition containing only 15 mol% TiO_2. As such, the deviation of the extent of the solid solution reported by different authors is thought to be due to this sensitivity of the system to excessively slow cooling rates and/or small temperature fluctuations. In summary, this work emphasises that a high level of control of sintering temperature and cooling profile is needed in order to form the most promising single-phase materials which contain maximum Ti-contents with low Y-contents which lie at the edge of the solid solution.

3.1.2. Conductivity behaviour

Contraction of the solid solution due to insufficient control of sintering conditions may have significant influence on the resultant conductivity behaviour. To emphasise the severity of this problem, the bulk conductivity behaviour of a single-phase sample of composition $Y_{0.2}Ti_{0.18}Zr_{0.62}O_{1.9}$ air quenched from 1500 °C was compared to a sample of the same composition air quenched from 1400 °C. Note that this composition represents the limit of the solid solution at 1500 °C. Fig. 3 shows that the sample air quenched from the lower temperature of 1400 °C is no longer of a single phase but clearly exhibits the presence of $Y_2Ti_2O_7$. Fig. 4 reveals that the bulk ionic conductivity of the phase pure 1500 °C sample is significantly lower than that of the phase-impure sample sintered at 1400 °C. To test reproducibility, the 1500 °C sample was resintered for 12 h at 1400 °C and air quenched. Fig. 4 shows that this resintered sample now exhibits enhanced bulk conductivity comparable to the initial 1400 °C sample. This validates the observation that contraction of the solid solution due to poor synthesis control may lead to the formation of secondary phases and an overestimation of the level of ionic conductivity. The presence of $Y_2Ti_2O_7$ as a secondary phase can be described by the relation

$$Y_{0.2}Ti_{0.18}Zr_{0.62}O_{1.9} \rightarrow \tfrac{1}{2}xY_2Ti_2O_7 + Y_{0.2-x}Ti_{0.18-x}Zr_{0.62}O_{1.9-3.5x}, \quad (1)$$

which leads to the parent cubic fluorite phase becoming more Zr-rich, as can be described by

$$\frac{Zr}{Y}=\frac{0.62}{0.2-x} \quad \text{and} \quad \frac{Zr}{Ti}=\frac{0.62}{0.18-x}. \quad (2)$$

That is the Zr/Y ratio and the Zr/Ti ratio both increase with increasing quantities (x) of the secondary-phase $Y_2Ti_2O_7$. From previous literature studies, it is known that an increase in either of these ratios leads to an increase in ionic conductivity [1–6,9–13], and can, therefore, explain

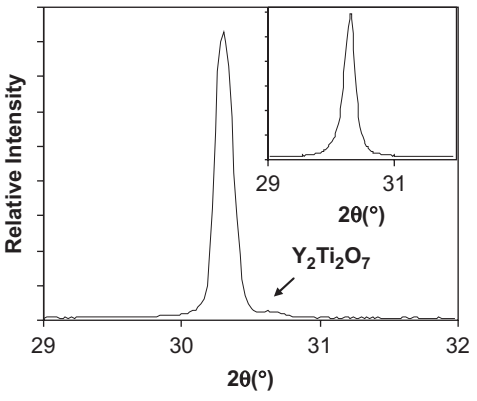

Fig. 3. X-ray diffractogram of the composition $Y_{0.2}Ti_{0.18}Zr_{0.62}O_{1.9}$ air quenched from 1400 °C showing contraction of the cubic solid solution and the presence of $Y_2Ti_2O_7$ as a secondary phase. Inset shows sample quenched from 1500 °C.

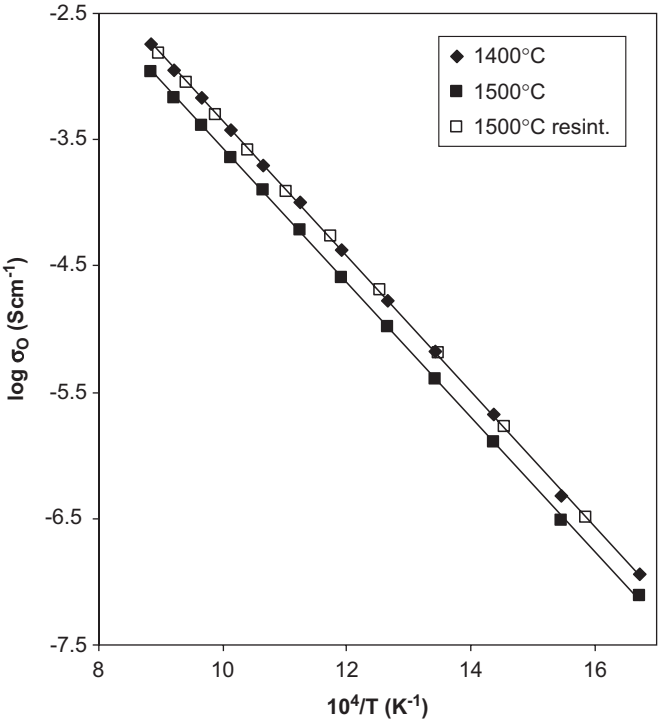

Fig. 4. The temperature dependence of bulk ionic conductivity in air of samples of $Y_{0.2}Ti_{0.18}Zr_{0.62}O_{1.9}$ air quenched from 1500 and 1400 °C. Reproducibility is demonstrated by re-sintering the 1500 °C sample at 1400 °C for 12 h and air quenching.

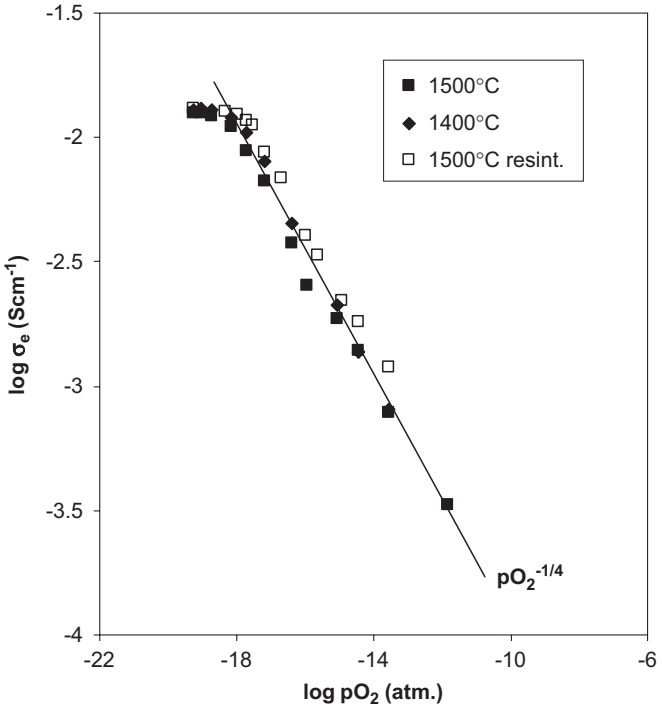

Fig. 5. The pO_2 dependence of electronic conductivity of samples of $Y_{0.2}Ti_{0.18}Zr_{0.62}O_{1.9}$ air quenched from 1500 and 1400 °C. Reproducibility is demonstrated by re-sintering the 1500 °C sample at 1400 °C for 12 h and air quenching.

the observed conductivity behaviour in this case. Overestimation of the level of ionic conductivity due to insufficient processing control may help to explain the disparity of current bulk conductivity data in the literature for samples lying at the very edge of the solid solution. Electronic conductivity is calculated by the equation

$$\sigma_e = \sigma_T - \sigma_o, \quad (3)$$

where σ_T is the total conductivity and σ_o is the ionic conductivity taken as being equal to the total conductivity measured in air. The influence of the solid solution contraction on the electronic conductivity is shown in Fig. 5 to be less severe with similar values of electronic conductivity shown by each sample regardless of thermal history.

In summary, the formation of a multiphase mixture due to contraction of the phase field of the cubic defect fluorite solid solution leads to a significant increase in the bulk ionic conductivity of samples lying at the edge of the solid solution. Extension of research to the study of multiphase compositions lying beyond the edge of the cubic solid solution may, therefore, offer an interesting new approach with which to obtain high levels of mixed conductivity from materials in the system ZrO_2–TiO_2–Y_2O_3. An example of this suggestion is work by Worrell [5] on composition $Y_{0.148}Ti_{0.185}Zr_{0.667}O_{1.926}$, a composition beyond the edge of the cubic solid solution, which demonstrates how this multiphase material may offer lower overpotential losses than that offered by

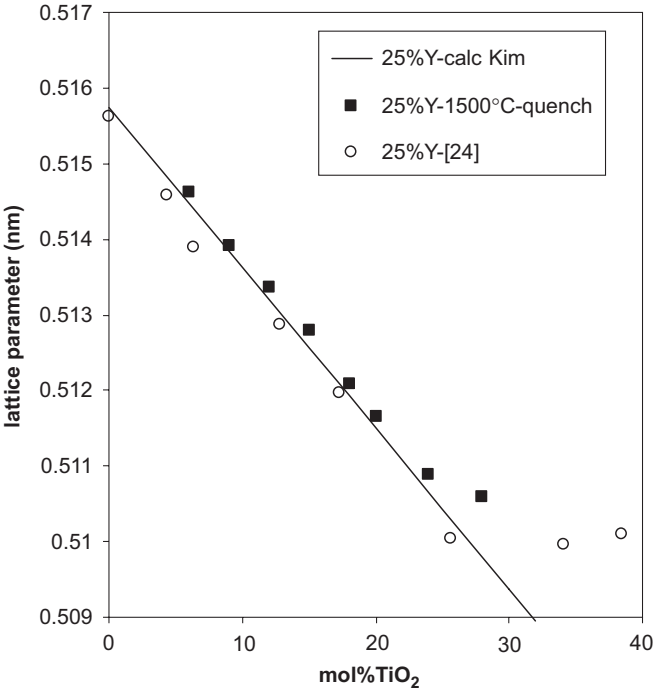

Fig. 6. Composition dependence of lattice parameter for compositions containing 25 mol% $YO_{1.5}$ air quenched from 1500 °C as a function of Ti-content and compared to literature data from Kobayashi et al. [24]. Lattice parameter is also calculated using the relation suggested by Kim [16].

current Ni-cermet anodes when tested as an electrode material for SOFC.

3.2. $Zr_{0.75-x}Ti_xY_{0.25}O_{2-\delta}$ (25 mol% $YO_{1.5}$)

Fig. 6 plots composition dependence of lattice parameter for compositions containing 25 mol% $YO_{1.5}$ as a function of Ti-content. Data from Kobayashi et al. [24] and Vegard behaviour predicted from the empirical relation of Kim [16] are also presented. A close correlation between all data sets is observed. The Kim relation appears to still hold at this dopant level. The limit of the cubic solid solution is observed to be in the region of 25 mol% TiO_2 for both experimental sets of data. This is a higher level of TiO_2 solubility for this $YO_{1.5}$ concentration than that of 15 mol% TiO_2 predicted from the phase diagram of Feighery et al. [14] which was not determined by the Vegard slope method for this Y-content.

4. Conclusions

The cubic defect fluorite-phase limits in the system ZrO_2–TiO_2–Y_2O_3 have been reassessed for compositions containing 20 and 25 mol% $YO_{1.5}$. Measured lattice parameters show good agreement with those calculated from the Kim relation and deviation from Vegard's law accurately places the limit of the solid solution at 18 and 25 mol% TiO_2 for values of 20 and 25 mol% $YO_{1.5}$, respectively, at 1500 °C. Discrepancies in current literature data have been suggested to be due to temperature fluctuations and/or differences in cooling rates. These factors lead to shrinkage of the cubic defect fluorite-phase field. One can interpret this by assuming that firing at higher temperature and/or fast cooling contributes to the prevention of ordering in the cation lattice and the formation of the pyrochlore phase. Contraction of the phase field by poor synthesis control may lead to erroneously high values of bulk ionic conductivity whilst values of electronic conductivity are less affected.

References

[1] H. Arashi, H. Naito, Solid State Ion. 53 (1992) 436.
[2] S.S. Liou, W.L. Worrell, Appl. Phys. A 49 (1992) 25.
[3] T. Lindegaard, C. Clausen, M. Mogensen, in: F.W. Poulsen, J.J. Bentzen, T. Jacobson, E. Skou, M.J.L. Ostergaard (Eds.), Proceedings of the 14th Riso International Symposium on Material Science, 1993, p. 117.
[4] S. Tao, J.T.S. Irvine, J. Solid State Chem. 165 (12–18) (2002) 12.
[5] W.L. Worrell, in: T.A. Ramanarayanan, W.L. Worrell, M. Mogensen (Eds.), Ionic and Mixed Conducting Ceramics IV, vol. 28, Electrochemical Society, Pennington, NJ, 2001, p. 75.
[6] D.P. Fagg, A.J. Feighery, J.T.S. Irvine, J. Solid State Chem. 172 (2003) 277.
[7] D. Skarmoutsos, P. Nikolopoulos, F. Tietz, I.C. Vinke, Solid State Ion. 170 (3–4) (2004) 153.
[8] M. Mori, Y. Hiei, H. Itoh, G.A. Tompsett, N.M. Sammes, Solid State Ion. 160 (1–2) (2003) 1.
[9] A. Kaiser, A.J. Feighery, D.P. Fagg, J.T.S. Irvine, Ionics 4 (1998) 215.
[10] W.L. Worrell, Y. Uchimoto, P. Han, in: Ionic and Mixed Conducting Ceramics III, vol. 97-24, Electrochemical Society, Pennington, NJ, 1998, p. 329.
[11] J.T.S. Irvine, A.J. Feighery, D.P. Fagg, S. García-Martín, Solid State Ion. 136 (2000) 879.
[12] M.T. Colomer, P. Durán, A. Caballero, J.R. Jurado, Mater. Sci. Eng. A 229 (1997) 114.
[13] L.S.M. Traqueira, T. Pagnier, F.M.B. Marques, J. Eur. Ceram. Soc. 17 (1997) 1019.
[14] A.J. Feighery, J.T.S. Irvine, D.P. Fagg, A. Kaiser, J. Solid State Chem. 143 (1999) 273.
[15] M.T. Colomer, J.R. Jurado, J. Solid State Chem. 165 (2002) 79.
[16] D.-J. Kim, J. Am. Ceram. Soc. 72 (8) (1989) 1415.
[17] H. Yokokawa, T. Horita, N. Sakai, M. Dokiya, J. Van Herle, S.G. Kim, Denki Kagaku 64 (6) (1996) 690.
[18] J.T.S. Irvine, D.P. Fagg, J. Labrincha, F.M.B. Marques, Catal. Today 38 (4) (1997) 467.
[19] R.D. Shannon, Acta Crystallogr. A 32 (1976) 751.
[20] D.W. Strickler, W.G. Carlson, J. Am. Ceram. Soc. 48 (6) (1965) 286–289.
[21] V.S. Stubican, R.C. Hink, S.P. Ray, J. Am. Ceram. Soc. 61 (1–2) (1978) 17–21.
[22] H.G. Scott, J. Mater. Sci 10 (9) (1975) 1527.
[23] J.S. Hong, A.V. Virkar, J. Am. Ceram. Soc. 78 (2) (1995) 433.
[24] K. Kobayashi, K. Kato, K. Terabe, S. Yamagughi, Y. Iguchi, J. Ceram. Soc. Japan 106 (9) (1998) 860.